# FERRITE PLANAR CIRCUIT IN MICROWAVE IC

Tanroku Miyoshi and Shinji Goto
Department of Electronic Engineering, Kobe University
Kobe, Japan

## Abstract

The main subject of this paper is the analysis of an arbitrarily-shaped, triplate ferrite planar circuit. The term "analysis" denotes here the determination of the circuit parameters of the equivalent multiport. It is shown that a computer analysis based upon a contour-integral solution of the wave equation offers an efficient tool in the design of the ferrite planar circuit. Examples of this analysis are also described.

## 1. Introduction

The ferrite planar circuit to be discussed in general in this paper is the planar circuit[1] using ferrite slabs as dielectric material, magnetized perpendicular to the ground conductors. The planar circuit is defined as an electrical circuit having dimensions comparable to the wavelength in two directions, but much less thickness in one direction. Therefore, the electromagnetic fields with no variation in one direction are considered in the planar circuit. From this point of view, not only the stripline circulator[2] consisting of a disk-shaped resonator but also the periphery mode(edge-guided mode) devices[3], which essentially require wide striplines and then have always tapered sections, are considered to be included in this circuit category.

The main subject of this paper is the analysis of an arbitrarily-shaped, triplate ferrite planar circuit. The term "analysis" denotes here the determination of the circuit parameters of the equivalent multiport. It is shown that a computer analysis based upon a contour-integral solution of the wave equation offers an efficient tool in the design of the ferrite planar circuit. Examples of this analysis are also described.

## 2. Basic Equation

The model to be considered is as follows. An arbitrarily-shaped, thin conducting center plate is sandwiched by two ferrite slabs magnetized perpendicular to the conducting plate and assumed to be excited symmetrically with respect to the upper and lower ground conductors. There are several coupling ports as shown in Fig.1 and the rest of the periphery is assumed to be open-circuited. The xy coordinates and the z axis, respectively, are set parallel and perpendicular to the conductors.

When the spacing d is much smaller than the wavelength and the ferrite substrates filling the space is homogeneous and linear, only the field components $E_z$, $H_x$ and $H_y$ with no variation along the z axis are considered. It is deduced directly from Maxwell's equation that the following equation dominates the electromagnetic fields in the ferrite planar circuit.

$$( \nabla_T^2 + \omega^2 \varepsilon \mu_{eff} )V=0 \tag{1}$$

where

$$\nabla_T^2=\frac{\partial^2}{\partial x^2}+\frac{\partial^2}{\partial y^2} \quad , \quad \mu_{eff}=\frac{\mu^2-\kappa^2}{\mu}$$

Here V denotes the rf voltage of the center conductor with respect to the ground conductors. The effective permeability $\mu_{eff}$ is given by $\mu$ and $\kappa$ which are the diagonal and off-diagonal coefficients of permeability tensor for magnetization in the z direction. The sign of $\mu_{eff}$ depends both on the operation frequency and on the internal magnetic field.

At a coupling port, the following boundary condition must hold:

$$j\frac{\kappa}{\mu}\frac{\partial V}{\partial t} + \frac{\partial V}{\partial n} = -j\omega\mu_{eff}\, di_n \tag{2}$$

where $i_n$ is the surface current density normal to the periphery C and $\partial/\partial n$ and $\partial/\partial t$, respectively, are the normal and tangential derivatives on C.

At most of the periphery where the coupling ports are absent, no current is assumed to flow at the edge of the center conductor in the direction normal to the edge, that is, $i_n=0$. Actually, however, the fringing magnetic fields are always present. A simple correction for it is to expand the periphery outwards by $0.447d\times K$ (K=0.4) in advance of the analysis. The coefficient K was determined by comparing the measured resonant frequencies for the various ferrite planar resonators with the theoretical values, which were computed by the Rayleigh-Ritz variational method* assuming that the circuits were lossless. As an example, the magnetically tuning characteristics of a square resonator are shown in Fig.2. It is shown in Fig.2 that if the effects of fringing fields are taken into account as indicated previously, the measured resonant frequencies are in good agreement with the calculated values especially above ferrimagnetic resonance because the higher the applied magnetic field, the smaller the influence of the magnetic loss. The computed amplitude and phase distribution of the proper rf voltage in the square resonator are also shown in Fig. 3 for the fundamental mode. The field patterns are found to be rotating to the right with time as are in the disk resonator. It is also found that when $\mu_{eff}<0$, the fields are somewhat concentrated along the periphery.

## 3. Computer Analysis

When we introduce the Green's function G, the rf voltage $V_p$ at a point P in the circuit is given by a line integral:

$$V_p=\int_C\{-j\omega\mu_{eff}\, di_n G + V(j\frac{\kappa}{\mu}\frac{\partial G}{\partial t} - \frac{\partial G}{\partial n})\}dt \tag{3}$$

We should use the different types of the Green's functions for Eq.(1) according to the sign of $\mu_{eff}$.

When $\mu_{eff}>0$, $G=H_0^{(2)}(kr)/4j$ is used as the freespace Green's function. From Eq.(3) the rf voltage at a point upon the periphery is found to satisfy the following equation.

$$V_M=\frac{1}{2j}\int_C\{j\omega\mu_{eff}\, dH_0^{(2)}(kr)(-i_n) + k(\cos\theta-j\frac{\kappa}{\mu}\sin\theta)H_1^{(2)}(kr)V_L\}dt \tag{4}$$

In this equation $H_0^{(2)}$ and $H_1^{(2)}$ are the zeroth order and first order Hankel functions of the second kind,

* Polynomial approximation was used for the functional I given by

$$I=\iint_D(|\nabla_T V|^2-\omega^2\varepsilon\mu_{eff}|V|^2)dS + j\frac{\kappa}{\mu}\int_C V^*\frac{\partial V}{\partial t}\,dt$$

which has its stationary condition(Euler equation) (1) and

$$j\frac{\kappa}{\mu}\frac{\partial V}{\partial t} + \frac{\partial V}{\partial n} =0 \qquad \text{on C}$$

respectively. The variable r denotes distance between points M and L represented by s and $s_0$, respectively, and $\theta$ denotes the angle made by the straight line from point M to point L and the normal at point L as shown in Fig.1. If the current density injected upon the periphery is known, Eq.(4) becomes a second kind Fredholm integral equation in terms of the rf voltage.

For numerical calculation we divide the periphery into N incremental sections and set N sampling points at the center of each section as shown in Fig.4. When we assume that the magnetic and electric field intensities are constant over each width of the sections, the above integral equation results in a matrix equation:

$$\sum_{j=1}^{N} u_{ij} = \sum_{j=1}^{N} h_{ij} \qquad (i=1,2,\cdots N) \tag{5}$$

where

$$u_{ij}=\delta_{ij}-\frac{k}{2j}\int_{W_j}\{\cos\theta-j\frac{\kappa}{\mu}\sin\theta\}H_1^{(2)}(kr)dt_j$$

$$h_{ij}=\begin{cases}\dfrac{\omega\mu_{eff}\,d}{4}\dfrac{1}{W_j}\displaystyle\int_{W_j}H_0^{(2)}(kr)dt_j & (i\neq j)\\[2ex] \dfrac{\omega\mu_{eff}\,d}{4}\{1-\dfrac{2j}{\pi}(\log\dfrac{kW_i}{4}-1+\gamma)\} & (i=j)\end{cases} \tag{6}$$

$\gamma=0.5772\cdots$: Euler's constant

and $I_j=-2i_nW_j$ represents the total current flowing into the j-th port. The formulas $u_{ij}$ and $h_{ij}$ in Eq.(6) have been derived assuming that the i-th section is straight. From the above relations, the impedance matrix of the equivalent N-port is obtained as

$$Z = U^{-1}H \tag{7}$$

where $U^{-1}$ denotes the inverse matrix to U. Then, the element of the impedance matrix is given as

$$Z_{ij} = \frac{1}{\det U}\begin{vmatrix} u_{11}\cdots \overset{i}{\underset{\downarrow}{h_{1j}}}\cdots u_{1N} \\ \vdots \quad\quad \vdots \quad\quad \vdots \\ u_{N1}\cdots h_{Nj}\cdots u_{NN}\end{vmatrix} \tag{8}$$

When the circuit has not coupling port, detU=0 gives the resonant frequency.

When $\mu_{eff}<0$, $G=(K_0(hr)+j\pi I_0(hr))/2\pi$ may be a suitable Green's function for Eq.(1), where $h=\omega\sqrt{\varepsilon|\mu_{eff}|}$ and $I_0$ and $K_0$ is the zeroth order modified Bessel functions of the first and second kind, respectively. In this case the elements of matrices U and H in Eq.(7) are found to be

$$u_{ij}=\delta_{ij}-\frac{h}{\pi}\int_{W_j}(\cos\theta-j\frac{\kappa}{\mu}\sin\theta)(K_1-j\pi I_1)dt$$

$$h_{ij}=\begin{cases}\dfrac{j\omega\mu_{eff}\,d}{2\pi}\dfrac{1}{W_j}\displaystyle\int_{W_j}(K_0+j\pi I_0)dt & (i\neq j)\\[2ex] -\dfrac{j\omega\mu_{eff}\,d}{2\pi}\{(\log\dfrac{hW_i}{4}+\gamma-1)-j\pi\} & (i=j)\end{cases} \tag{9}$$

## 4. Examples of Analysis

As examples of the computer analysis, the resonant frequencies of a disk-shaped circuit were computed first for the check of the computation accuracy. Since detU=0 is never realized for real frequency due to the computation error, we define the frequency which gives the minimum of $|\det U|$ as the eigenvalue. The variation of $|\det U|$ is shown as a function of frequency $F(GH_z)$ in Fig.5 for $\mu_{eff}>0$, which shows the first(F=4.35), the second(F=5.31), the third(F=6.05) and the fourth(6.85) minima. The calculated eigenvalues were compared with the theoretical values which should be given by the roots of

$$J_n'(ka)-\frac{\kappa n J_n(ka)}{\mu\ ka}=0 \qquad (n=0,\ \pm1,\ \pm2\cdots)$$

$$I_n'(ha)-\frac{\kappa n I_n(ha)}{\mu\ ha}=0 \qquad (n=1,\ 2\ \cdots) \tag{10}$$

and then it was verified that the computation errors were within 2.0 per cent for the number of the sampling points N=33.

Next, the characteristics of the Y-junction stripline circulator were computed as shown in Fig.6. The circulator performance in Fig.6 is for the above ferrimagnetic resonance point of circulation. Here the internal magnetic field is 3700 Oe and N=33. At this applied magnetic field, the resonant frequencies of +1 and -1 modes are $5.5GH_z$ and $4.9GH_z$, respectively, which shows that the frequency of operation is not midway between +1 and -1 mode resonant frequencies but out of the region. This is believed due to the operation far from the degeneracy of $\pm1$ modes, that is, a greater separation of the modes, and the great influence of higher modes which results from the heavy coupling to the striplines.

Fig.7 shows the rf voltage distribution along the periphery at the center frequency in the circulator performance for N=33. The solid and broken curves show the relative magnitude and phase of the rf voltage along the periphery, respectively. The distribution of the amplitude is not sinusoidal, as might be expected, with much shallower minimum between the input and output ports and a greater distortion in the vicinity of the ports.

## 5. Conclusion

We have presented the computer analysis based upon a contour-integral equation of an arbitrarily-shaped ferrite planar circuit. It is expected in the future that such an approach will be useful in the design and analysis of microwave integrated circuits on ferrite substrates. Furthermore, we add that the circuit parameters of the ferrite planar circuit can be also determined in general by expanding the rf voltage in terms of orthonomal eigenfunctions. However, such an analysis based upon eigenfunction expansion has been omitted in this paper for space limitations and will be reported elsewhere.


## Acknowledgement

The authors wish to thank Prof. T.Okoshi of University of Tokyo for his encouragement and S.Yamaguchi of Kobe University for his excellent assistance in some of the computer programming involved in this work.


## References


1. T.Okoshi and T.Miyoshi,"The planar circuit - an approach to microwave integrated circuitry," IEEE Trans.MTT, Vol.MTT-20, No.4, pp.245-252, Apr.1972.
2. H.Bosma,"On stripline Y-circulation at UHF," IEEE Trans.MTT, Vol.MTT-12, No.1, pp.61-72, Jan.1964.
3. M.E.Hines,"Reciprocal and nonreciprocal modes of propagation in ferrite stripline and microstrip devices," IEEE Trans.MTT, Vol.MTT-19, No.5, pp.442-451, May 1971.


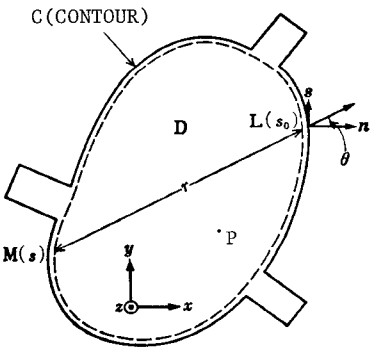


Fig.1 Center conductor of a ferrite planar circuit and symbols used in the integral equation.

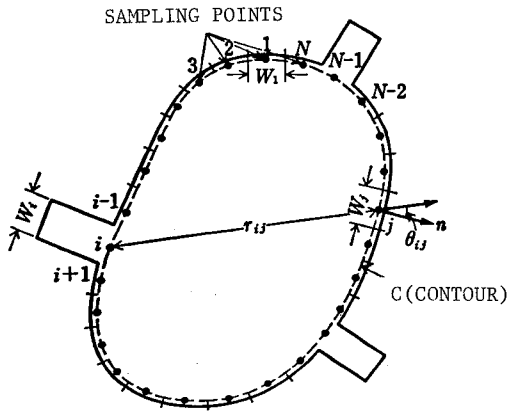


Fig.2 Symbols used in the computer analysis.

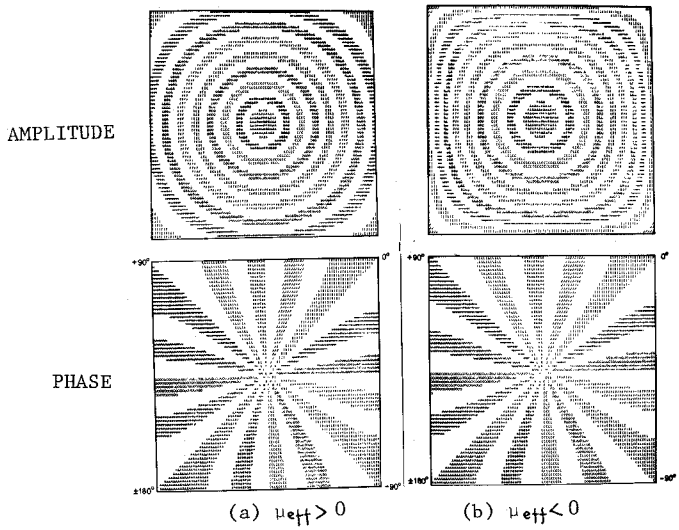


Fig.4 Computed distribution of the rf voltage in the square resonator for the fundamental mode. Equal amplitude(upper) and phase(lower) lines are shown for (a) $\mu_{eff} > 0$, the applied magnetic field $H_0$= 1300 Oe and (b) $\mu_{eff} < 0$, $H_0$=2300 Oe.

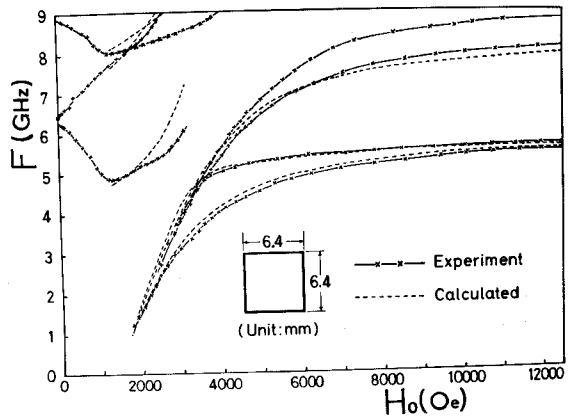


Fig.3 Magnetically tuning characteristics of a square resonator. The broken curve were calculated by the polynomial approximation of order 5, taking the effects of fringing fields into account. The ferrimagnetic substrates of the saturation magnetization $4\pi M_S$=1300Gauss, the linewidth $\Delta H$= 68 Oe and the dielectric constant $\varepsilon$=15.6 were used in the experiment.

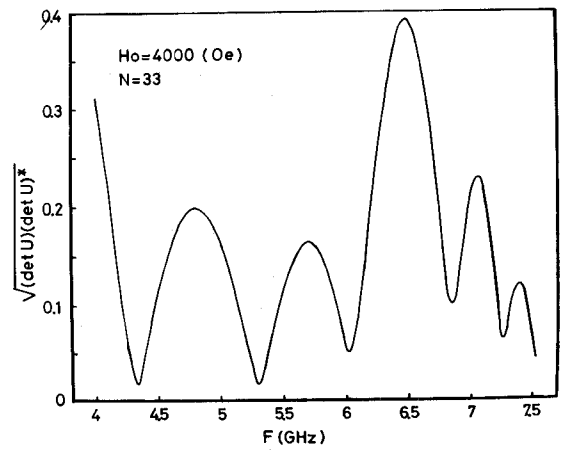


Fig.5 The variation of |detU| as a function of frequency of a disk-shaped circuit for N=33 when $\mu_{eff} > 0$.

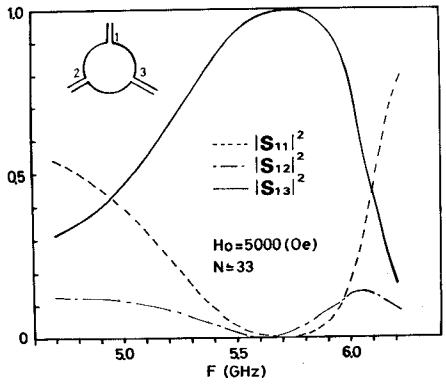


Fig.6 Computed performance of a stripline Y-junction circulator coupled by striplines of 50 ohm at the above resonance point of circulation for N=33.

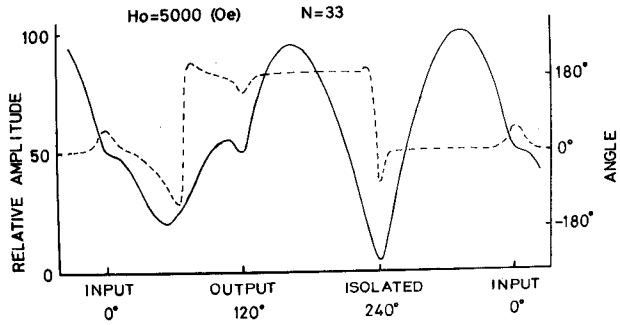


Fig.7 Computed rf voltage distribution along the periphery of the stripline circulator at the center frequency in the performance shown in Fig.6. Solid curve indicates the amplitude given in arbitrary unit and broken curve is the phase line.